ELSEVIER

Journal of Alloys and Compounds 452 (2008) 268–272

Journal of ALLOYS AND COMPOUNDS

www.elsevier.com/locate/jallcom

Bulk metallic glass formation in a ternary Ti–Cu–Ni alloy system

X.F. Wu [a,*], Z.Y. Suo [a], Y. Si [a], L.K. Meng [a], K.Q. Qiu [b]

[a] *Faculty of Materials and Chemical Engineering, Liaoning Institute of Technology, 169 Shiying Street, Jinzhou 121001, PR China*
[b] *School of Materials Science and Engineering, Shenyang University of Technology, 58 South Xinghua Street, Shenyang 110023, PR China*

Received 20 April 2006; received in revised form 28 October 2006; accepted 1 November 2006
Available online 28 November 2006

Abstract

The glass-forming ability (GFA), thermal stability and mechanical properties of ternary $Ti_{50}Cu_{50-x}Ni_x$ ($x = 5$, 8 and 11) alloys have been investigated. The results show that bulk metallic glass (BMG) with a diameter of at least 2 mm was successfully fabricated by conventional Cu-mold casting method for $Ti_{50}Cu_{42}Ni_8$ alloy, which exhibits a wide undercooled liquid region ΔT_x of 56 K, a high reduced glass transition temperature T_{rg} of 0.57 and compressive fracture strength of 2008 MPa. This new found ternary BMG could be regarded as a good candidate for developing a new series of BMGs.

Keywords: Ti–Cu–Ni; Glass-forming ability; Bulk metallic glass; Mechanical properties

1. Introduction

Over the past few decades, bulk metallic glasses (BMGs) have attracted extensive interests due to their unique physical, chemical and mechanical properties attributed to the random atomic configurations. Many kinds of BMGs have been developed in Pd- [1], Re (La, Nd)- [2,3], Zr- [4], Ti- [5], Ni- [6], Cu- [7], and Mg-based [8] systems. Among them, much more attention was paid to Ti-based amorphous alloys because of their high specific strength and relatively low cost.

Ti-rich amorphous alloys with a supercooled liquid region during heating have been reported in Ti–Be–Zr [9], Ti–Ni–Si [10], Ti–Nb–Si–B [11], Ti–Ni–Cu [12], Ti–Ni–Cu–Al [13] and Ti–Zr–Ni–Cu [14]. However, no BMGs are formed in these alloys due to their poor glass-forming ability (GFA), so that a fully amorphous structure was available only in the form of ribbon. Recently, Zhang and Inoue [5] reported that a fully amorphous rod of a $Ti_{50}Cu_{20}Ni_{24}Sn_3B_1Si_2$ alloy with a diameter of 1 mm was fabricated by injection casting. Kim et al. [15] reported a $Ti_{50}Cu_{25}Ni_{15}Sn_3Be_7$ BGM with the maximum diameter of 3 mm, by partial replacement of Cu by Be as well as Ti by Zr; the diameters of glassy rods could be increased from 3 to 5 mm for $Ti_{45}Cu_{25}Ni_{15}Sn_3Be_7Zr_5$ alloy and to 8 mm for $Ti_{40}Zr_{25}Ni_8Cu_9Be_{18}$ alloy, respectively [16]. More recently, BMGs with a diameter of 2 mm have been reported in the more complex multi-component Ti–Cu–Ni–Al–Si–M–B (M = Sc, Hf, Ta and Nb) system [17].

No Ti-based BMGs with sample binary or ternary components have been prepared and only with complex multi-components so far. The fabrication of BMGs in a simple binary or ternary alloy system is significant to understand the GFA of alloys. Amorphous phase formation by rapid solidification processes has been reported in $Ti_{50}Ni_{25}Cu_{25}$ [12] and $Ti_{50}Cu_{45}Ni_5$ [13] alloys. In addition, early study showed that the GFA for ternary Ti–Ni–Cu system is good for Cu-rich compositions and poor for Ni-rich compositions [18]. Therefore, it is expected that there is the possibility to form BGMs in a ternary Ti-rich–Cu-rich–Ni system. More recently, we have successfully fabricated BMG with a diameter of at least 2 mm in a ternary Ti–Cu–Ni alloy system by conventional Cu-mold casting method. This paper intends to present the GFA, thermal stability, mechanical properties and fracture behavior of Ti–Cu–Ni bulk glassy alloys.

2. Experimental procedure

Ingots with nominal composition of $Ti_{50}Cu_{50-x}Ni_x$ ($x = 5$, 8 and 11 at.%) were prepared by arc melting the mixture of pure metals (Ti, Cu and Ni) with a purity of more than 99.9% under a Ti-gettered Ar atmosphere. To ensure homogeneity of the samples, the ingots were remelted several times. For the

* Corresponding author. Tel.: +86 416 4199758; fax: +86 416 4199758.
E-mail address: hgd901@126.com (X.F. Wu).

0925-8388/$ – see front matter © 2006 Elsevier B.V. All rights reserved.
doi:10.1016/j.jallcom.2006.11.010

bulk samples, the 60 mm length cylindrical rods with different diameters were prepared by pouring liquid metal, which was melted using induction furnace, through a quartz nozzle into a copper mold under certain argon pressure as well as purified argon atmosphere. In addition, ribbon samples were prepared by melt spinning and the ribbons approximately 25 μm in thickness and 3 mm in width were obtained.

The structure of samples was checked by X-ray diffraction (XRD) with Cu Kα radiation. Thermal stability associated with glass transition, supercooled liquid region and crystallization were examined by continuous heating in a differential thermal analysis (Perkin-Elmer Pyris Diamond TG/DTA) at a heating rate of 0.67 K/s under flowing high purity N_2 (200 ml/min). The DTA data were transformed into differential scanning calorimeter (DSC) data by using the Perkin-Elmer-edited computer program. Al_2O_3 pans were used and the mass of sample was between 20 and 30 mg. Compression experiments were carried out on an MTS-type axial-torsional load frame at room temperature. The compressive strain rate was $3.0 \times 10^{-4}\ s^{-1}$. Six rods with the same diameter and composition were compressed.

3. Results

Fig. 1 shows XRD patterns obtained from the as-cast rods with different diameters prepared by the copper-mold casting for $Ti_{50}Cu_{50-x}Ni_x$ ($x = 5$, 8 and 11) alloys. For the rod samples with a diameter of 2 mm, the XRD patterns from the alloy $x = 8$ consists only of a broad peak, with no evidence of any crystalline Bragg peaks within the detectable limitation of the XRD, while a few sharp diffraction peaks corresponding to crystalline phases superimposed on the broad amorphous peaks are

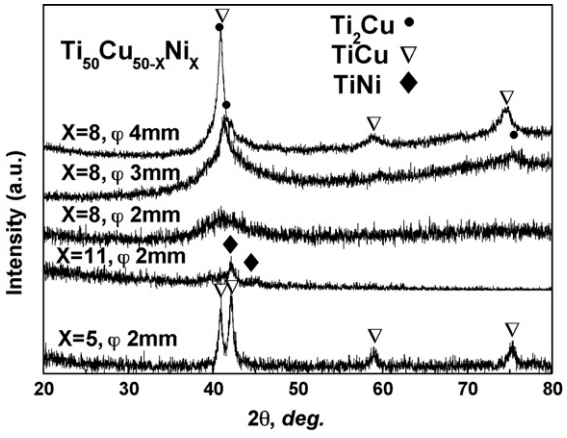

Fig. 1. XRD patterns obtained from the as-cast rods with different diameters for $Ti_{50}Cu_{50-x}Ni_x$ ($x = 5$, 8 and 11) alloys.

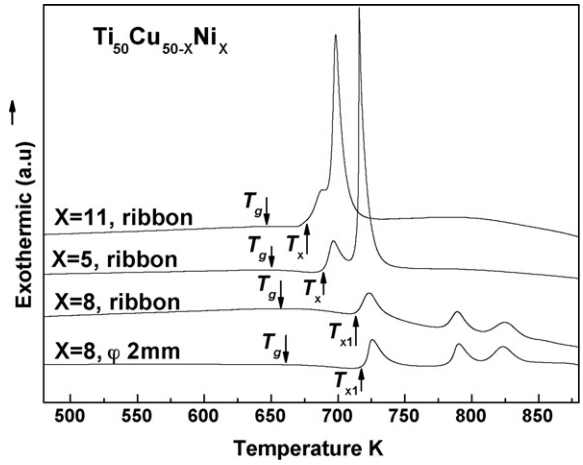

Fig. 3. DSC traces of the melt-spun $Ti_{50}Cu_{50-x}Ni_x$ glassy alloys ($x = 5$, 8 and 11) and as-cast $Ti_{50}Cu_{42}Ni_8$ glassy alloy.

observed for the other alloys, indicating that the $Ti_{50}Cu_{42}Ni_8$ alloy is fully amorphous and the others are partially amorphous with a significant fraction of crystalline phases. The crystalline phases were identified as TiCu and TiNi for the $Ti_{50}Cu_{45}Ni_5$ and $Ti_{50}Cu_{39}Ni_{11}$ alloys, respectively. As the rod diameter increased to 3 mm, the broad amorphous peak from the $Ti_{50}Cu_{42}Ni_8$ alloy became sharp; a small amount of phase identified as Ti_2Cu precipitates in the amorphous matrix, and then some sharp peaks from Ti_2Cu and TiCu phases appeared in the broad peak matrix with the further increase of the rod diameter to 4 mm. Thus, when Ni content increases to 8 at.%, the precipitation of TiCu phase in the $Ti_{50}Cu_{45}Ni_5$ alloy can be avoided, and more addition leads to the precipitation of TiNi phase. Based on these observations, it is therefore concluded that bulk metallic glass can be formed in a ternary Ti–Cu–Ni alloy system and the maximum diameter to form the metallic glass lies between 2 and 3 mm for the $Ti_{50}Cu_{42}Ni_8$ alloy. Moreover, no visible crystalline phase was found in the SEM taken from the edge and central region of the cross-section of the 2 mm rod sample of the alloy, as shown in Fig. 2(a and b).

Fig. 3 shows DSC traces of the melt-spun $Ti_{50}Cu_{50-x}Ni_x$ glassy alloys ($x = 5$, 8 and 11) and as-cast $Ti_{50}Cu_{42}Ni_8$ glassy alloy during continuous heating with a heating rate of 0.67 K/s. All curves exhibit a clear endothermic heat event character-

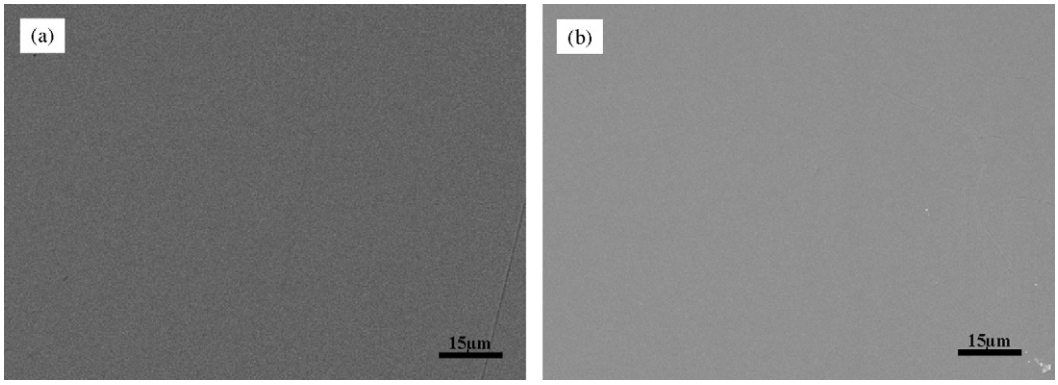

Fig. 2. Scanning electron micrograph taken from (a) the edge and (b) central region of the cross-section of the as-cast $Ti_{50}Cu_{42}Ni_8$ 2-mm-diameter rod.

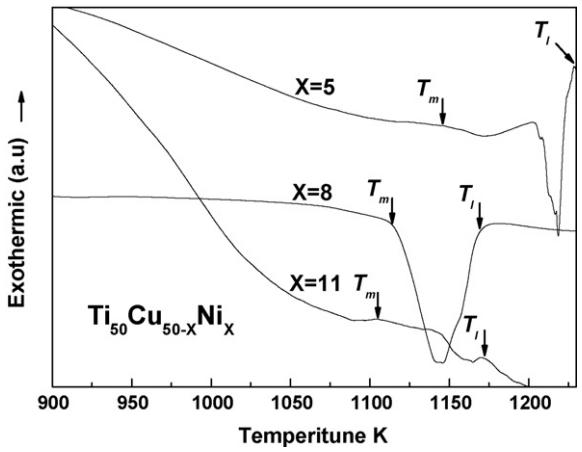

Fig. 4. High-temperature DSC traces of the melt-spun $Ti_{50}Cu_{50-x}Ni_x$ glassy alloys ($x = 5$, 8 and 11).

istic of the glass transition, followed by a broad supercooled liquid region and then exothermic reactions due to crystallization, which is different from that of binary $Ti_{50}Cu_{50}$ glassy alloy which crystallizes directly from the amorphous solid [13]. The glass temperature, T_g, the onset temperature of the crystallization, T_x, for the $Ti_{50}Cu_{45}Ni_5$ and $Ti_{50}Cu_{39}Ni_{11}$ alloys or the onset temperature of the first crystallization, T_{x1}, for the $Ti_{50}Cu_{42}Ni_8$ alloy, the supercooled liquid region, $\Delta T_x = T_x - T_g$ or $= T_{x1} - T_g$ are listed in Table 1. With increasing Ni content (x) from 5 to 8, both T_g and T_x increased from 650 to 657 K and 689 to 713 K, respectively, and then decreased to 646 and 677 K, respectively, with increasing x from 8 to 11. As a result, ΔT_x for $x = 5$, 8 and 11 were 39, 56 and 31 K, respectively, and maximum ΔT_x of 56 K was obtained in the $Ti_{50}Cu_{42}Ni_8$ alloy. Also, it can be noticed that a large exothermic peak with a small shoulder due to crystallization is observed for the alloy $x = 5$ and 11 during continuous heating. However, three exothermic reactions caused by crystallization appear in the DSC trace of the $Ti_{50}Cu_{42}Ni_8$ alloy, indicating a change of crystallization behavior with x. From the Fig. 3, one can also see that the cast $Ti_{50}Cu_{42}Ni_8$ alloy prepared into 2 mm-diameter rod also crystallized by three-step process. The T_g and onset temperature of first, second and third crystallization, T_{x1}, T_{x2} and T_{x3} of the rod are almost the same as those of the melt-spun ribbons, which have full glassy structure for $Ti_{50}Cu_{42}Ni_8$ alloy. In addition, the amount of heat released during the first, second and third crystallization of the rod is also almost the same as that of the fully glassy ribbons, respectively. These results again confirm the as-cast glassy structure of this alloy as concluded from its XRD pattern.

Fig. 4 shows typical melting curves for the melt-spun ribbons corresponding to $x = 5$, 8 and 11, obtained by extending the heating temperature in DSC measurement until the melting of the alloys took place at a heating rate of 0.33 K/s. It can be seen that Ni content significantly affects the melting behaviors of these alloys. The solidus temperature T_m and liquidus temperature T_l are assumed to be the onset and end temperatures of the endothermic melting, respectively. The alloy with $x = 5$ showed a rather high T_l (~1228 K) and a melting process consisting of

Table 1
The glass transition temperature T_g, onset temperature of primary crystallization T_x, supercooled liquid region ΔT_x ($= T_x - T_g$), solidus temperature T_m, liquidus temperature T_l, reduced glass temperature T_{rg} ($= T_g/T_l$) and γ ($= T_x/(T_g + T_l)$) for $Ti_{50}Cu_{50-x}Ni_x$ ($x = 5$, 8 and 11) alloys

Alloys	T_g (K)	T_x (K)	ΔT_x (K)	T_m (K)	T_l (K)	T_{rg}	γ
$Ti_{50}Cu_{45}Ni_5$	650	689	39	1146	1228	0.529	0.367
$Ti_{50}Cu_{42}Ni_8$	657	713	56	1114	1168	0.563	0.391
$Ti_{50}Cu39Ni_{11}$	646	677	31	1105	1170	0.552	0.373

one major endothermic event, followed by a minor secondary event, resulting in a large melting range of about 82 K, which indicate that this alloy is at off-eutectic composition. In the DSC scan of the alloy at $x = 8$, the T_l was lowered by about 60 K compared with the alloy at $x = 5$. The melting process showed the nearly single endothermic peak with a small shoulder and narrow melting temperature ranges of about 54 K, suggesting that this alloy is quite close to a ternary eutectic composition. When x is further increased to11, the T_l remains almost the same value of about 1170 K as the alloy at $x = 8$ but multiple events appeared again during its melting process, resulting in the decrease of the T_m and the increase of the temperature interval of melting up to about 65 K. A critical parameter to determine the GFA of an alloy is the reduced glass transition temperature, T_{rg}, defined as the glass transition temperature T_g divided by the liquidus temperature T_l ($T_{rg} = T_g/T_l$). Another GFA criterion proposed recently by Lu and Liu is the parameter γ [19], where $\gamma = T_x/(T_g + T_l)$. Taken the data of the T_l for the alloy $x = 5$, 8 and 11, T_{rg} and γ for the alloys were obtained, which was also given in Table 1. The T_{rg} and γ values of the $Ti_{50}Cu_{42}Ni_8$ alloy are 0.573 and 0.395, which is the largest value, respectively, for the present three Ti-based amorphous alloys, and is consistent with an improved GFA of the alloys. Therefore, both T_{rg} and γ should be good criterions for the GFA in the present Ti–Cu–Ni alloy system, and the $Ti_{50}Cu_{42}Ni_8$ alloy which could be prepared into an amorphous cast rod exhibits higher GFA than the other Ti-based alloys only into ribbons.

Fig. 5 shows the quasistatic compressive stress–strain curve at room temperature for the as-cast amorphous $Ti_{50}Cu_{42}Ni_8$ alloy

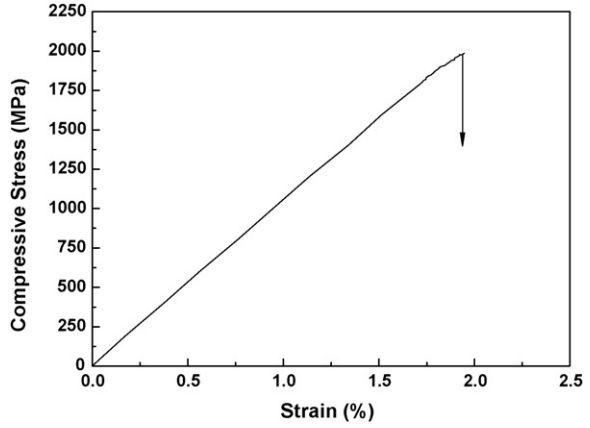

Fig. 5. The compressive stress–strain curve under the constant cross-head speed condition of an strain rate of 3.0×10^{-4} s^{-1} at room temperature for amorphous $Ti_{50}Cu_{42}Ni_8$ rods.

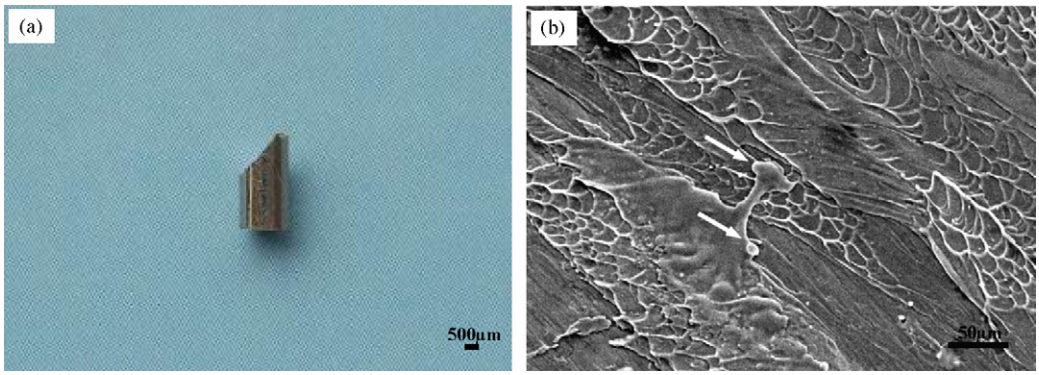

Fig. 6. Scanning electron micrography of (a) the external appearance of the failed amorphous $Ti_{50}Cu_{42}Ni_8$ rod and (b) its fracture surface.

rod with a diameter of 2 mm and a length of 4 mm. As other metallic glasses, the curve only displays an initial elastic deformation behavior with almost no plasticity at room temperature. At the same time, the sample shows outstanding mechanical properties, namely a favorable combination of high fracture strength of 2008 MPa and low Young's modulus of 100 GPa, indicating that very high values of elastic energy can be stored in the material.

Fig. 6(a and b) shows the micrograph of fractured specimen and fracture surface, respectively, of the amorphous $Ti_{50}Cu_{42}Ni_8$ alloy. Under compressive loading, the fracture takes place along the maximum shear plane, inclined by about 45° to the direction of the applied load indicating dominance of shear stress in the failure process. Further observations show that the fracture surface showed a well-developed vein pattern. Also, it can be noticed that local melting as evidenced by the formation of "liquid droplets" takes place during shear deformation as marked by arrows in Fig. 6(b). This well-developed vein and local melting pattern is consistent with the observations in most metallic glasses [20], which is attributed to local softening or melting induced by the decrease of viscosity or local adiabatic heating within the shear band.

4. Discussion

The present results show that the GFA is significantly improved when Cu is partially replaced by Ni in the binary $Ti_{50}Cu_{50}$ alloy. Ternary $Ti_{50}Cu_{42}Ni_8$ BMG with diameter of at least 2 mm is successfully fabricated by conventional Cu-mold casting method. To our knowledge, the BMG may be the first one discovered in ternary Ti–Cu–Ni alloy system so far. The alloys with high glass-forming ability has been recognized to satisfy three empirical rules [21], i.e., (1) multi-component systems consisting of more than three elements, (2) significant atomic mismatches above 12% among the main three constituent elements, and (3) negative heats of mixing among the main elements. Although Ni and Cu have nearly same atomic radius, the negative mixing heat of Ni–Ti pair (−35 kJ/mol) is larger than that of Cu–Ti pair (−9 kJ/mol) [22]. Thus, the local atomic structure of the liquid, tending to form local clusters consisting of Ni–Ti atomic pairs in ternary Ti–Cu–Ni alloys can lead to an increase in the degree of dense random packed atomic configurations and make the rearrangement of the constituent elements on a long-range scale difficult. This favors the stabilization of the liquid phase with respect to competing crystalline phases during solidification.

It is well known that lowering the liquidus temperature and altering the alloy composition up to the eutectic or near the eutectic are key steps in fabricating BMGs. The Ti–Cu binary system has a binary eutectic point at composition$Ti_{56}Cu_{44}$ with a binary eutectic temperature T_E of 1233 K. The ternary alloys reported in this paper were developed based on this binary eutectic composition. The $Ti_{50}Cu_{42}Ni_8$ alloy has a low liquidus temperature T_l and composition close to ternary eutectic point (Fig. 4), which can avoid the precipitation of the primary TiCu phase in the $Ti_{50}Cu_{45}Ni_5$ alloy with the smaller amount of Ni (5 at.%) or the primary TiNi phase in the $Ti_{50}Cu_{39}Ni_{11}$ alloy with the larger amount of Ni (11 at.%) (Fig. 1). Thus, the structure of the liquid of the $Ti_{50}Cu_{42}Ni_8$ alloy is more stable than those of $Ti_{50}Cu_{45}Ni_5$ and $Ti_{50}Cu_{39}Ni_{11}$ alloys which exhibit a high T_l and off-eutectic composition attributed to the precipitation of the primary TiCu and TiNi phase during solidification, respectively (Fig. 4), resulting in the improvement of GFA and the forming of BMG. As mentioned above, the amorphous phase of the $Ti_{50}Cu_{42}Ni_8$ alloy crystallized through three-step process. This crystallization mode is significantly different from those for the other two Ti-based glassy alloys studied in this paper and $Ti_{50}Cu_{45}M_5$ (M = Cu, Ni, Co, Fe or Si) glassy alloys studied in Ref. [5], which crystallize through a single exothermic reaction. It is necessary to investigate the different crystallizing modes for further understanding the GFA of ternary Ti–Cu–M (Ni) alloy system. More work in this direction is underway.

From above results, one can see that the ternary Ti-rich–Cu-rich–Ni alloy system is a good candidate for developing new bulk metallic glasses. It is expected that an addition of additional elements to the Ti–Cu–Ni alloys will improve the glass-forming ability even further. In fact, fully amorphous rods with a diameter of at least 3 mm from quinary Ti–Cu–Ni–Sn–Zr alloy have recently been fabricated in our group, and these results will be published shortly elsewhere.

5. Conclusion

Ternary $Ti_{50}Cu_{42}Ni_8$ BMG with a diameter of at least 2 mm was successfully fabricated by conventional Cu-mold casting method. The undercooled liquid region ΔT_x and reduced glass

transition temperature T_{rg} of the BMG are 56 and 0.57 K, respectively. Compared with the $Ti_{50}Cu_{45}Ni_5$ and $Ti_{50}Cu_{39}Ni_{11}$ metallic glasses, the $Ti_{50}Cu_{42}Ni_8$ metallic glass crystallized in a multiple-stage process. In addition, The BMG exhibits compressive fracture strength of 2008 MPa. All the ΔT_x, T_{rg} and new parameter γ have a close relationship with the GFA and thermal stability of the ternary Ti–Cu–Ni alloy system.

Acknowledgements

Funding by the Natural Science Foundation of Liaoning Province under Grant no. 20032137 is gratefully acknowledged.

References

[1] A. Inoue, N. Nishiyama, H. Kimura, Mater. Trans. JIM 38 (1997) 179.
[2] A. Inoue, T. Zhang, T. Masumoto, Mater. Trans. JIM 31 (1990) 425.
[3] A. Inoue, T. Zhang, A. Takeuchi, W. Zhang, Mater. Trans. JIM 37 (1996) 636.
[4] A. Peker, W.L. Johnson, Appl. Phys. Lett. 63 (1993) 2342.
[5] T. Zhang, A. Inoue, Mater. Sci. Eng. A 304–306 (2001) 771.
[6] S. Yi, T.G. Park, D.H. Kim, J. Mater. Res. 15 (2000) 2425.
[7] X.H. Lin, W.L. Johnson, J. Appl. Phys. 78 (1995) 6514.
[8] A. Inoue, K. Kato, T. Zhang, S.G. Kim, T. Masumoto, Mater. Trans. JIM 32 (1991) 609.
[9] L.E. Tanner, R. Ray, Scripta Metall. Mater. 11 (1977) 783.
[10] D.E. Polk, A. Calka, B.C. Giessen, Acta Mater. 26 (1978) 1097.
[11] A. Inoue, T. Masumoto, C. Suryanarayana, J. Phys. 41C (1980) 8758.
[12] T. Zhang, A. Inoue, T. Masumoto, Mater. Sci. Eng. A181–A182 (1994) 1423.
[13] A. Inoue, N. Nishiyama, K. Amiyarn, T. Zhang, T. Masumoto, Mater. Lett. 19 (1994) 131.
[14] K. Amiya, N. Nishiyama, A. Inoue, T. Masumoto, Mater. Sci. Eng. A 179–180 (1994) 692.
[15] Y.C. Kim, W.T. Kim, D.H. Kim, Mater. Trans. JIM 43 (2002) 1243.
[16] Y.C. Kim, W.T. Kim, D.H. Kim, Mater. Sci. Eng. A 375–377 (2004) 127.
[17] M.X. Xia, H.X. Zheng, J. Liu, C.L. Ma, J.G. Li, J. Non-Cryst. Solids. 351 (2005) 3747.
[18] B.S. Murty, M.M. Rao, S. Ranganathan, Mater. Sci. Eng. A 196 (1995) 237.
[19] Z.P. Lu, C.T. Liu, Acta Mater. 50 (2002) 3501.
[20] H.A. Bruck, A.J. Rosakis, W.L. Johnson, J. Mater. Res. 11 (1996) 503.
[21] A. Inoue, Mater. Trans. JIM 36 (1995) 866.
[22] F.R. De Boer, R. Boom, W.C.M. Mattens, A.R. Miedema, A.K. Niessen, Cohesion in Metals, North-Holland, Amsterdam, 1988.